

Article

Structural characterization of antiviral compounds from medicinal plants against SARS-CoV-2: A computational study

Fateme Mollaamin^{1,*}, Majid Monajjemi²¹ Department of Biomedical Engineering, Faculty of Engineering and Architecture, Kastamonu University, Kastamonu 37150, Turkey² Department of Chemical Engineering, Central Tehran Branch, Islamic Azad University, Tehran 496969191, Iran* **Corresponding author:** Fateme Mollaamin, fmollaamin@kastamonu.edu.tr

CITATION

Mollaamin F, Monajjemi M.
Structural characterization of
antiviral compounds from medicinal
plants against SARS-CoV-2: A
computational study. *Molecular &
Cellular Biomechanics*. 2025; 22(3):
1114.
<https://doi.org/10.62617/mcb1114>

ARTICLE INFO

Received: 16 December 2024

Accepted: 6 February 2025

Available online: 24 February 2025

COPYRIGHT



Copyright © 2025 by author(s).
Molecular & Cellular Biomechanics
is published by Sin-Chn Scientific
Press Pte. Ltd. This work is licensed
under the Creative Commons
Attribution (CC BY) license.
[https://creativecommons.org/licenses/
by/4.0/](https://creativecommons.org/licenses/by/4.0/)

Abstract: Natural products are vital and rich sources for plant-based drugs and new medicines. Recent studies emphasize secondary metabolites of natural products due to their unparalleled pharmacological action, biological activity and high usage cost. In addition, with the progress of investigation on biosynthesis and molecular metabolism of medicinal plants, the procedures for illustrating the pharmacological impacts and biological activity of these compounds are firmly developing. The principal section of the translation process is the synthesis of secondary metabolites. In this work, seven flavonoids, namely *apigenine-7-glucoside*, *catechin*, *demethoxycurcumine*, *kaempferol*, *naringenin*, *oleuropein* and *quercetin* have also previously been reported to inhibit RNA (Ribonucleic acid) replication and viral translation. Among applied extracted phytochemicals in this investigation, oleuropein's has exhibited lowest Gibbs free energy of -1206.893×10^3 kcal/mol with high dipole moment of 6.1962 Debye. In this study, we combine CAM-B3LYP-D3 and NQR (Nuclear quadrupole resonance) for evaluating plant-derived anti-SARS-CoV-2 compounds through computationally estimating the binding mechanisms and thermodynamic stability of seven flavonoids against SARS-CoV-2's TMH (Tyrosine 160–Methionine 161–Histidine 162) active site.

Keywords: virus; natural products; Covid19; antiviral secondary metabolites; mechanobiology

1. Introduction

While commonly used antivirals often show limited efficacy and serious adverse effects, herbal extracts have been in use for medicinal purposes since ancient times and are known for their antiviral properties and more tolerable side effects [1–6]. Thus, naturally based pharmacotherapy may be a proper alternative for treating viral diseases. With that in mind, various pharmaceutical formulations and delivery systems including micelles, nanoparticles, nanosuspensions, solid dispersions, microspheres and crystals, self-nanoemulsifying and self-microemulsifying drug delivery systems have been developed and used for antiviral delivery of natural products [7–11]. These diverse technologies offer effective and reliable delivery of medicinal phytochemicals [12–16].

Many chemical compounds found in natural resources supply important directions for medicine products and can participate in antiviral therapy. The compounds extracted from natural resources have an essential function in medication exploration and the improvement of novel antiviral remedies. Natural products have emerged as a promising frontier in the research for novel antiviral treatments [17–19].

Various phytochemicals were isolated, purified, and identified from the crude extracts of alkaloids, terpenes, flavonoids, various glycosides, and proteins.

Compounds with antiviral activity are present in many plants, e.g., rutin, a flavonoid glycoside common in different plants, is effective against avian influenza virus, HSV-1 (Herpes Simplex Virus), HSV-2, and parainfluenza-3 virus [20–22].

Quercetin, an aglycone of rutin, is a phytochemical abundant in plants and may diminish the replication of many viruses such as highly pathogenic influenza virus, rhinovirus, dengue virus type-2, poliovirus, adenovirus, Epstein-Barr virus, Mayaro virus, Japanese encephalitis virus, and respiratory syncytial virus. Its ability to limit the activity of some heat shock proteins produced by cells in response to exposure to stress which were involved in nonstructural protein 5A-mediated viral of internal ribosome entry site translation is one well-known mechanism [23].

Apigenin (4,5,7-trihydroxyflavone), an aglycone of the flavone class, is found in many plants and has broad antiviral activities against enterovirus-71, foot and mouth disease virus, African swine fever virus, and influenza A virus. Many flavonoids of plant origin have known antiviral properties. For example, out of 22 different flavonoids, six phytochemicals including *apigenin*, *baicalein*, *biochanin A*, *kaempferol*, *luteolin*, and *naringenin* were active against the avian influenza virus in human lung epithelial cells through inhibiting nucleoprotein production [24].

Baicalin (the glucuronide of baicalein) was also active against a wide range of viruses, containing enterovirus, dengue virus, respiratory syncytial virus, Newcastle disease virus, human immunodeficiency virus, and hepatitis B virus, and different mechanisms were suggested for its antiviral actions. Baicalin inhibits the production of HBV (Hepatitis B virus), the templates for viral proteins and HBV-DNA synthesis, and decreases IL-6 and IL-8 production without affecting IP-10 levels [25].

Flavonoids contain a common phenylchromen-4-one scaffold which can be substituted with a phenyl ring at C2 or C3 to give the flavone and isoflavone backbone structure. In this article, we investigated *apigenine-7-glucoside*, *catechin*, *demethoxycurcumine*, *kaempferol*, *naringenin*, *oleuropein* and *quercetin* with similar structure extracted from *Goji berries*, *Green tea*, *Turmeric*, *Chinese cabbage*, *Citrus fruit*, *Olive* and *Chili pepper*, as the probable “anti-Covid19” receptor taken from natural products (**Table 1**).

Table 1. Medicinal ingredients of *apigenine-7-glucoside*, *catechin*, *demethoxycurcumine*, *kaempferol*, *naringenin*, *oleuropein* and *quercetin* as the probable anti-Covid19 receptor.

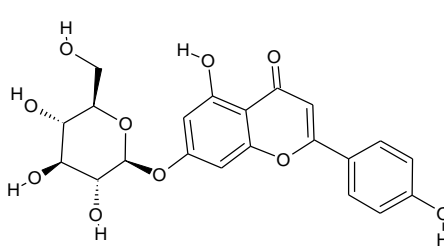

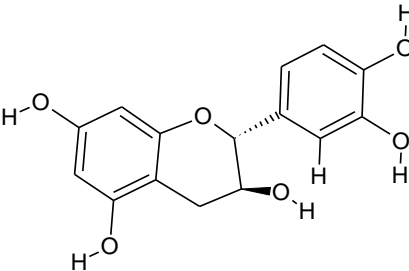

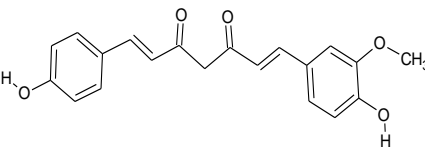

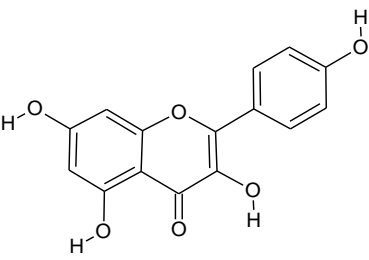

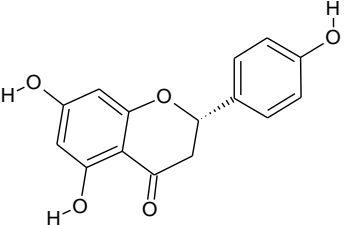

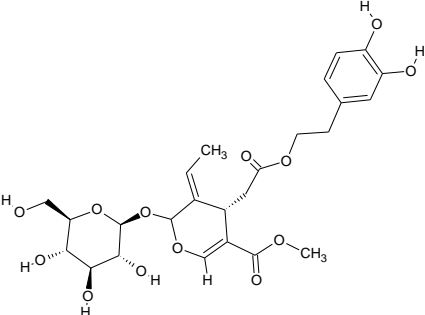

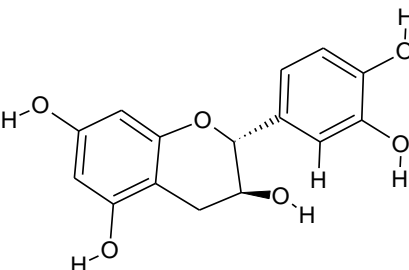
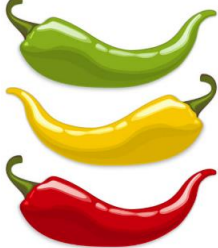
Ingredient	Chemical structure	Origin
<i>apigenine-7-glucoside</i>		<i>Goji berries</i> 

Table 1. (Continued).

Ingredient	Chemical structure	Origin
<i>Catechin</i>	 <p>The chemical structure of Catechin is a flavan-3-ol. It consists of a chromane ring system with hydroxyl groups at positions 2, 3, and 5 on the A-ring, and a catechol group at position 2 on the C-ring.</p>	<p><i>Green tea</i></p> 
<i>demethoxycurcumine</i>	 <p>The chemical structure of demethoxycurcumine is a polyphenolic compound. It features a central heptane chain with two enone groups and two phenolic rings. One phenolic ring has a methoxy group and a hydroxyl group, while the other has two hydroxyl groups.</p>	<p><i>Turmeric, Curcuma</i></p> 
<i>kaempferol</i>	 <p>The chemical structure of kaempferol is a flavonol. It consists of a chromone ring system with hydroxyl groups at positions 3, 5, and 7 on the A-ring, and a phenyl group at position 4 on the C-ring.</p>	<p><i>Chinese cabbage</i></p> 
<i>naringenin</i>	 <p>The chemical structure of naringenin is a flavanone. It consists of a chromone ring system with hydroxyl groups at positions 5 and 7 on the A-ring, and a p-coumaroyl group at position 4 on the C-ring.</p>	<p><i>Citrus fruit</i></p> 
<i>oleuropein</i>	 <p>The chemical structure of oleuropein is a complex polyphenolic compound. It features a flavanone core with a glucose moiety at position 7, a methyl group at position 2, and a hydroxyethyl ferulate moiety at position 4.</p>	<p><i>Olive</i></p> 
<i>quercetin</i>	 <p>The chemical structure of quercetin is a flavonol. It consists of a chromone ring system with hydroxyl groups at positions 3, 5, and 7 on the A-ring, and a catechol group at position 4 on the C-ring.</p>	<p><i>Chili pepper</i></p> 

The results of this research article conduct the scientists to discover the appropriate medications against Covid19 by quantum mechanics approaches to figure out the influence of H-bonding in various linkage through the natural products of *apigenine-7-glucoside*, *catechin*, *demethoxycurcumine*, *kaempferol*, *naringenin*, *oleuropein* and *quercetin* attached to the active site of “Covid19” protein (**Figure 1**). Given the challenges and possibilities of antiviral treatment, this research article provides verified data on the medicinal plants and related herbal substances with antiviral activity, as well as applied of these plant extracts and biologically active phytochemicals. This study aims to computationally evaluate the binding mechanisms and thermodynamic stability of seven flavonoids against the SARS-CoV-2 Tyr160–Met161–His162 (TMH) active site using DFT and NQR analyses.

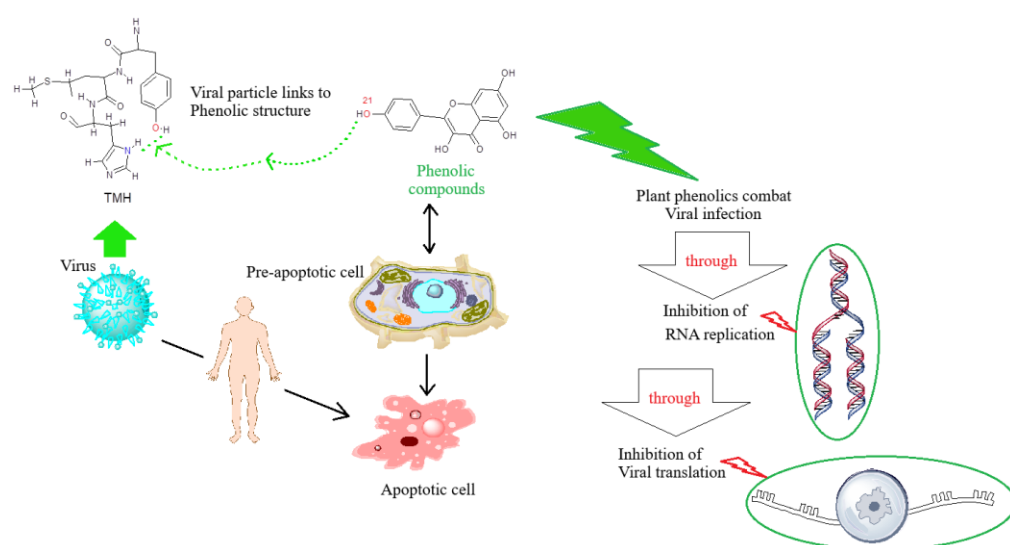


Figure 1. The connection of phenolic compounds as an “anti-Covid19” drug through O21 atom to TMH (Tyr160–Met161–His162) by H-bonding.

2. Materials and methods

In DFT, as it is applied for theoretical chemistry, the hybrid functional Becke 3-parameter Lee-Yang-Parr (B3LYP) is observed to propose the greatest contribution. A novel hybrid exchange–correlation functional as Coulomb-Attenuating Method with CAM-B3LYP is suggested which merges the hybrid qualities of B3LYP and the long-range correction [26]. Furthermore, in the DFT–D3 method of Grimme et al. [27], the following expression for the “Van Der Waals (vdW)-dispersion energy-correction term is used:

$$E_{\text{disp}} = -\frac{1}{2} \sum_{i=1}^{N_{\text{at}}} \sum_{j=1}^{N_{\text{at}}} \sum_L \left(f_{d,6}(r_{ij,L}) \frac{C_{6ij}}{r_{ij,L}^6} + f_{d,8}(r_{ij,L}) \frac{C_{8ij}}{r_{ij,L}^8} \right) \quad (1)$$

The dispersion coefficients C_{6ij} are geometry dependent as they are adjusted based on the local coordination surrounding atoms i and j . Thus, a series of quantum mechanical calculations using the DFT-D3 (Density Functional Dispersion Correction) method was performed for seven SARS-CoV-2 inhibitor complexes owing to discovering the minimized parameters of the best compounds of medicinal plant–

Tyr160–Met161–His162 medication design template with IR computations by Gaussian 16 revision C.01 program [28].

The junction of *apigenine-7-glucoside*, *catechin*, *demethoxycurcumine*, *kaempferol*, *naringenin*, *oleuropein* and *quercetin* attached to the active site of Covid19 protein was performed in this research article by building stable structures through the H-bonding. It was displayed that polarization functions on the pragmatic basis set in the calculation status represent us a significant success on the modeling/simulation theoretical steps [29–33]. Normal mode implement is the adjustment of harmonic potential wells by analytic approaches which hold the motion of all elements at the same time in the vibration time scale conducting to a natural illustration of vibrations in molecules [34–37]. Hence, the minimized structure of medicinal components-TMH clusters into the medication design was done through the active site of demonstrated “O, N, H” (**Figure 1**). Torsion angles were constrained using Gaussian 16’s [28] relaxed potential energy scan at the B3LYP/6–31G(d) level. Molecular docking was performed using AutoDock Vina v1.2.0 [38] with a grid box centered on TMH residues ($x = -0.2615$, $y = 0.3570$, $z = -4.4615$). Validation included RMSD calculations ($< 2 \text{ \AA}$) against co-crystallized ligands.

3. Results and discussion

3.1. Background: Viral-host interactions and flavonoid mechanisms

Viruses use the cellular passages and resources of their respective host cells to be alive and replicated. The method of viruses for applying the metabolic abilities of host cells for their own replication can differ. The most common metabolic alterations operated by viruses impact the central carbon metabolism of infected host cells, especially the tricarboxylic acid cycle, glycolysis and the pentose phosphate pathway. The upregulation of these procedures is targeted to enhance the reserve of amino acids, lipids and nucleotides because these metabolic products are vital for impressive viral replication. But this manipulation might impact multiple zones and regulatory mechanisms of host-cell metabolism, relating not only to the viruses but also to the kind of infected host cells. So, it pursued metabolic situations and reprogramming in various human organs, tissues and host cells which are desirable for sharp and continuous SARS-CoV-2 infection. This science may be essential for the progress of host-directed treatments [39–42].

The genome of SARS-CoV-2 carries information for four structural proteins, the spike glycoprotein, the envelope protein, the membrane protein, and the nucleocapsid protein for 16 non-structural proteins and for 9 small accessory proteins [43]. In fact, the viral proteins that may affect the metabolism of the infected host cells can be considered the entry of SARS-CoV-2 into host cells and the exit of intact virus particles [44]. Generally, phenols are discovered in all herb organs and are strong ingredients of legumes, fruits, cereals, and beverages. Some famous phenolic structures with resulting antiviral functions contain phenolic acids, tannins, and flavonoids [45].

In this article, phenolic compounds including *apigenine-7-glucoside*, *catechin*, *demethoxycurcumine*, *kaempferol*, *naringenin*, *oleuropein* and *quercetin* are the most

broadly spread secondary metabolites in plants and are synthesized as an adaptive reply to unpleasant situations [46].

Regarding survival strategy, plants' secondary metabolites are produced versus adverse status and perform physiological functions. It can be seen different parameters applied in characterizing the categorization of secondary metabolites in herbal products consisting of composition of elements, chemical structure, and their solubility in water or other solvents. The phenolic compounds indicate various phytochemical ingredients and pharmacological impacts against different viral compounds. The noticed mechanisms of operation of plant-extracted secondary metabolites versus viruses consisting of virus entry attachment, inhibition of viral replication, protein synthesis inhibition, modulation of the host's immune system, modulation of cellular signaling pathways, and direct virucidal activity (**Figure 1**).

The process of operation of phenols versus viruses is related to the kind of phenolic compound and the aimed virus. The phenols are famous to prevent viral infection of an aimed host cell in a diversity of paths [47,48], containing the disruption of the virus lipid bilayer covers and prohibiting viral linkage to the host cell [49]. In addition, the prevention of diverse viral protein activities includes the disconnection of the viral life cycle that inhibits the replication and liberation of the virus [50]. Furthermore, the molecular modeling method between active sites of medicinal ingredients jointed to the database amino acids fragment of Tyr160–Met161–His162 through hydrogen bonding formation which is a special type of dipole-dipole attraction between molecules was also used to predict the antiviral effects of medicinal plants against SARS-CoV-2 (**Figure 1**).

3.2. Chemical shielding insight through nuclear magnetic resonance spectrum

Nuclear magnetic resonance (NMR)-based metabolomics has many usages in natural science. Metabolomics can be applied in functional genomics to distinguish natural products from various origins and after various remedies. The principal benefit of NMR metabolomic analysis is the feasibility of recognizing metabolites by evaluating NMR data with references or by structure illustration [51,52]. The heterocyclic antiviral phytochemicals have approximately exhibited the equal manner from 20 to 300 ppm for different atoms of these phytochemicals (**Figure 2a–g**). The nuclear magnetic resonance spectrum displayed the steepest peak in 40 ppm and the fragile peaks of nuclear magnetic resonance have approximately in 100–200 ppm for all antiviral phytochemicals (**Figure 2a–g**).

The nuclear magnetic resonance analysis shows the critical points of the principal components of medicinal plants for binding to the Tyr160–Met161–His162 (TMH) due to producing the antivirus drugs, while each active atom of O and N as the electronegative atoms for binding to the H remarks the maximal shift in all steps in the NMR spectrum (**Figure 2a–g**).

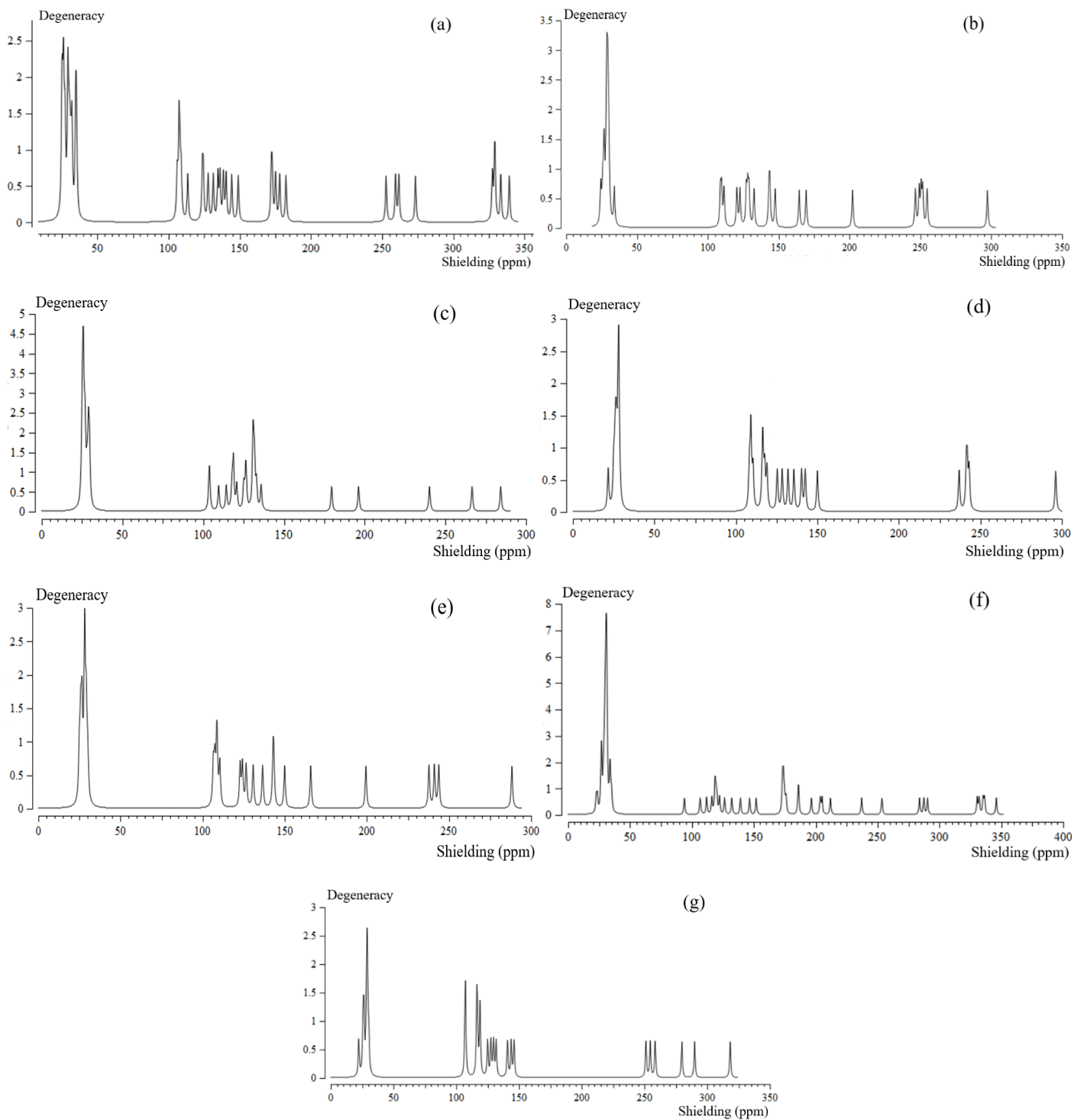


Figure 2. NMR spectra of: **(a)** apigenine-7-glucoside; **(b)** catechin; **(c)** demethoxycurcumine; **(d)** kaempferol; **(e)** naringenin; **(f)** oleuropein; **(g)** quercetin bonded to TMH (Tyr160–Met161–His162) COVID19.

3.3. Nuclear quadrupole resonance analysis

The nuclear quadrupole resonance (NQR) is attached to the “multipole expansion” in “Cartesian coordinates as [53–60]:

$$V(r) = V(0) + \left[\left(\frac{\partial V}{\partial x_i} \right) \Big|_0 \cdot x_i \right] + \frac{1}{2} \left[\left(\frac{\partial^2 V}{\partial x_i \partial x_j} \right) \Big|_0 \cdot x_i x_j \right] + \dots \quad (2)$$

After that, a simplification on the Equation (2), there are only the second derivatives related to the identical variable for the potential energy [53–60]:

$$U = -\frac{1}{2} \int_{\mathcal{D}} d^3 r \rho_r \left[\left(\frac{\partial^2 V}{\partial x_i^2} \right) \Big|_0 \cdot x_i^2 \right] = -\frac{1}{2} \int_{\mathcal{D}} d^3 r \rho_r \left[\left(\frac{\partial E_i}{\partial x_i} \right) \Big|_0 \cdot x_i^2 \right] = -\frac{1}{2} \left(\frac{\partial E_i}{\partial x_i} \right) \Big|_0 \cdot \int_{\mathcal{D}} d^3 r [\rho(r) \cdot x_i^2] \quad (3)$$

There are two parameters which must be gotten from NQR experiments: the quadrupole coupling constant, χ , and asymmetry parameter of the EFG tensor η :

$$\chi = e^2 Q q_{zz} / h \quad (4)$$

$$\eta = (q_{xx} - q_{yy}) / q_{zz} \quad (5)$$

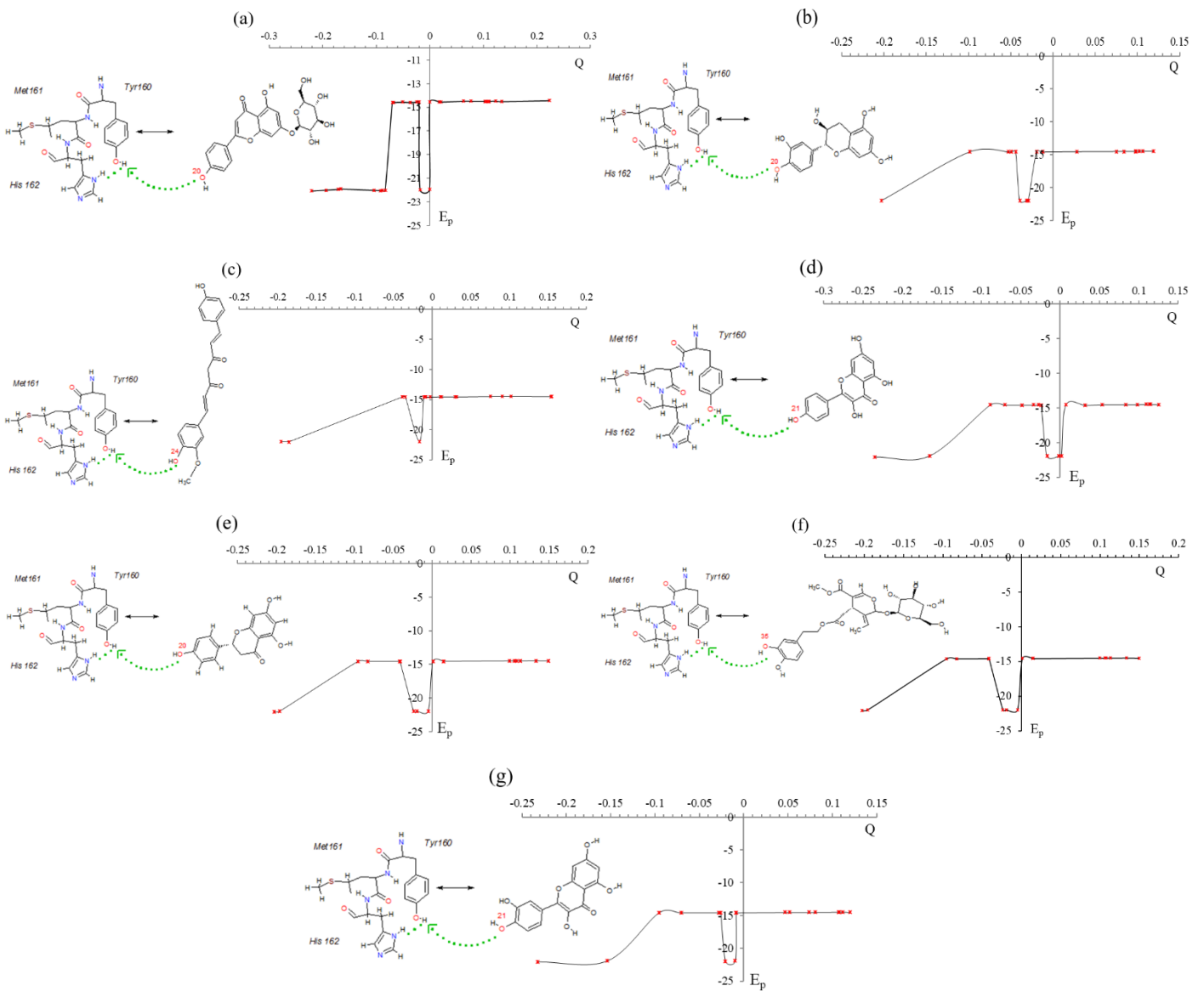


Figure 3. Electric potential (a.u.) versus Bader charge (e) through NQR calculation for: (a) *apigenine-7-glucoside*; (b) *catechin*; (c) *demethoxycurcumine*; (d) *kaempferol*; (e) *naringenin*; (f) *oleuropein*; (g) *quercetin* bonded to TMH (Tyr160–Met161–His162) COVID-19 active site.

The electric potential as the content of work energy through carrying over the electric charge from one status to another status in the being of electric field has been rated for *apigenine-7-glucoside*, *catechin*, *demethoxycurcumine*, *kaempferol*, *naringenin*, *oleuropein* and *quercetin* bonded to “TMH (Tyr160–Met161–His162) COVID-19” active site (**Figure 3a–g**).

In **Figure 3a–g**, it has been sketched the electric potential of nuclear quadrupole resonance for some atoms of in the linkage bond between *apigenine-7-glucoside*, *catechin*, *demethoxycurcumine*, *kaempferol*, *naringenin*, *oleuropein* and *quercetin* and TMH (Tyr160–Met161–His162) COVID19 active site which has been calculated by CAM-B3LYP–D3. In **Figure 3a–g**, it has been described the influence of each active atom of O and N as the electronegative atoms for binding to the H atom.

3.4. Thermodynamic properties analysis and infrared spectroscopy

The parameters extracted from thermodynamic calculations for *apigenine-7-glucoside*, *catechin*, *demethoxycurcumine*, *kaempferol*, *naringenin*, *oleuropein* and *quercetin* extracted from “*Goji berries*, *Green tea*, *Turmeric*, *Chinese cabbage*, *Citrus fruit*, *Olive* and *Chili pepper*”, was represented in **Table 2**.

Table 2. Thermodynamic parameters for *apigenine-7-glucoside*, *catechin*, *demethoxycurcumine*, *kaempferol*, *naringenin*, *oleuropein*, *quercetin* and *remdesivir* and its inhibitors (L) [61] using density functional theory method.

Phytochemicals	$\Delta E^{\circ} \times 10^{-3}$ (kcal/mol)	$\Delta H^{\circ} \times 10^{-3}$ (kcal/mol)	$\Delta G^{\circ} \times 10^{-3}$ (kcal/mol)	Reference Drug [61]	ΔG_{Bind} (kcal/mol) [61]	S° (Cal/K.mol)	Dipole moment (Debye)
<i>apigenine-7-glucoside</i>	-968.078	-968.077	-968.117	<i>remdesivir</i>	-85.532	134.625	5.4672
<i>catechin</i>	-638.496	-638.495	-638.530	L3	-79.556	116.702	4.2660
<i>demethoxycurcumine</i>	-711.496	-711.495	-711.531	L5	-75.170	119.571	4.4508
<i>kaempferol</i>	-637.052	-637.051	-637.084	L2	-87.618	109.232	3.1205
<i>naringenin</i>	-591.276	-591.275	-591.307	L7	-85.047	106.656	2.6658
<i>oleuropein</i>	-1206.850	-1206.849	-1206.893	L8	-80.029	147.632	6.1962
<i>quercetin</i>	-683.579	-683.578	-683.612	L12	-88.173	112.611	4.4357

The alteration in stability energy for folding spans in globular proteins have been measured as -1206.893×10^3 , -968.117×10^3 , -711.531×10^3 , -683.612×10^3 , -638.530×10^3 , -637.084×10^3 , and -591.307×10^3 kcal.mol⁻¹ for *oleuropein*, *apigenine-7-glucoside*, *demethoxycurcumine*, *quercetin*, *Catechin*, *kaempferol*, and *naringenin*, respectively. **Table 2** has shown the minimum Gibbs free energy consisting of -1206.893×10^3 kcal.mol⁻¹ for *oleuropein* versus dipole moment which can indicate the most stability of these structures of the antiviral natural medications. Moreover, infrared spectroscopy of major sesquiterpenes was performed due to CAM-B3LYP–D3 method (**Figure 4a–g**).

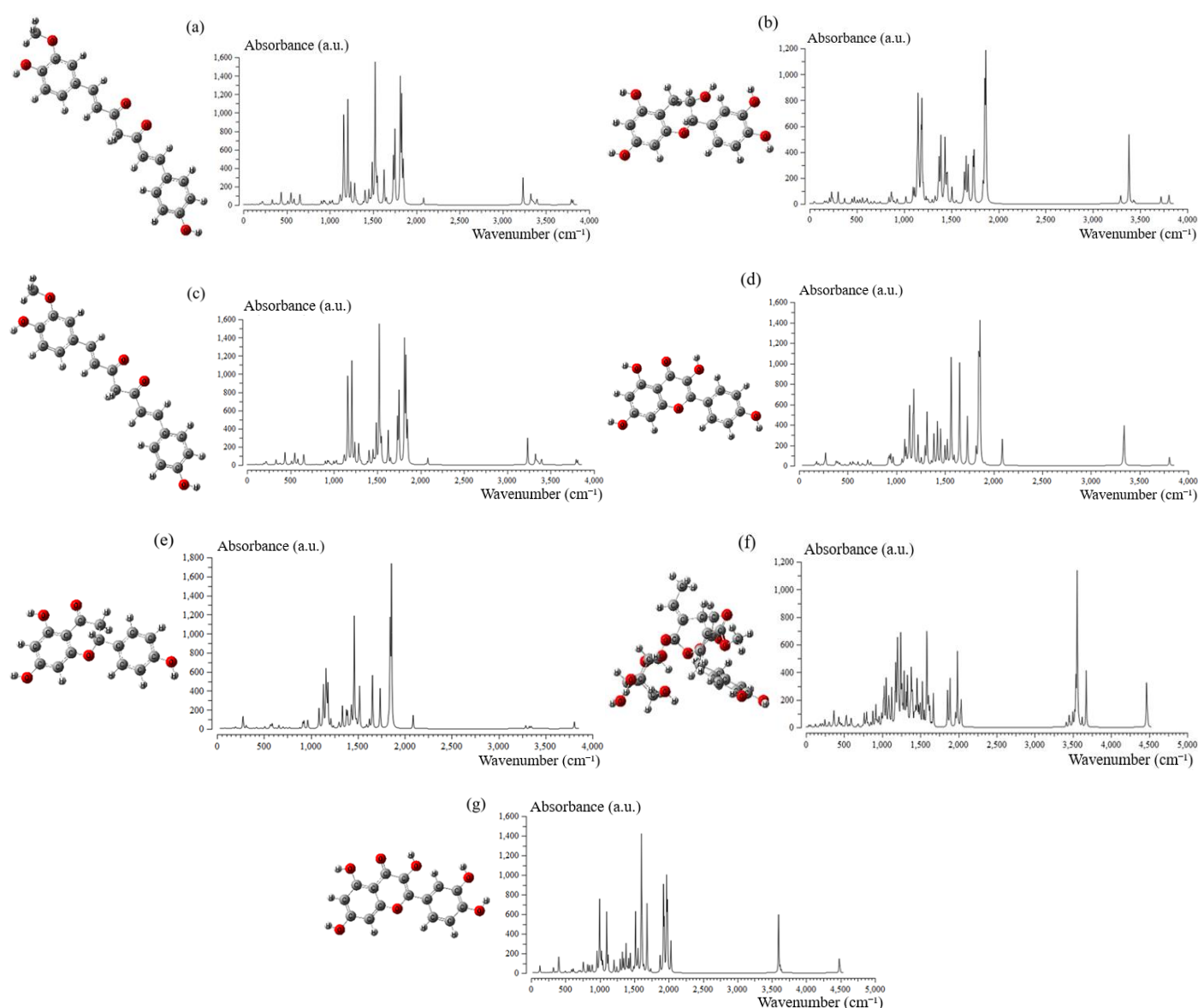


Figure 4. IR spectra of: (a) *apigenine-7-glucoside*; (b) *catechin*; (c) *demethoxycurcumine*; (d) *kaempferol*; (e) *naringenin*; (f) *oleuropein*; (g) *quercetin* to TMH (Tyr160–Met161–His162) through the drug design method.

The IR spectrum shows a frequency range $3600\text{--}3200\text{ cm}^{-1}$ that represents the O–H stretching vibration, which confirms the presence of phenolics. The peak under frequency ranges $3000\text{--}2850\text{ cm}^{-1}$ and $1680\text{--}1620\text{ cm}^{-1}$ represented C–H stretching vibration of alkanes containing aromatic compounds. The peak range $1680\text{--}1620\text{ cm}^{-1}$ indicated the --C=C-- stretching vibration, and confirmed the presence of alkenes. Presence of alcohol, esters and ethers are confirmed in frequency range $1320\text{--}1000\text{ cm}^{-1}$. This range showed C–O stretching vibration at 1049.28 cm^{-1} peak (**Figure 4a–g**).

3.5. Frontier orbitals

The Frontier orbitals have been estimated for some effective phytochemicals of *apigenine-7-glucoside*, *catechin*, *demethoxycurcumine*, *kaempferol*, *naringenin*,

oleuropein and *quercetin* extracted from “*Goji berries, Green tea, Turmeric, Chinese cabbage, Citrus fruit, Olive and Chili pepper*” (**Table 3**).

Table 3. The Frontier orbitals’ parameters (eV) of antiviral phytochemicals including *apigenine-7-glucoside, catechin, demethoxycurcumine, kaempferol, naringenin, oleuropein and quercetin*.

Molecule	E _{LUMO}	E _{HOMO}	ΔE = E _{LUMO} – E _{HOMO}
<i>apigenine-7-glucoside</i>	1.6751	-2.8819	4.557
<i>catechin</i>	3.1633	-2.6612	5.8245
<i>demethoxycurcumine</i>	1.1276	-2.4406	3.5682
<i>kaempferol</i>	1.6245	-2.7195	4.344
<i>naringenin</i>	1.9946	-3.0422	5.0368
<i>oleuropein</i>	2.3676	-0.9254	3.293
<i>quercetin</i>	1.3570	-2.5780	3.935

The “highest occupied molecular orbital energy (HOMO/eV)”, the “lowest unoccupied molecular orbital energy (LUMO/eV)” and “band energy gap ΔE (eV)” exhibited the “pictorial description of positive and negative areas” that are a vital agent for identifying the molecular nominations of antiviral phytochemicals (**Table 3**).

4. Conclusions

It is concluded that herbal medications owing to effective active phytoingredients may grow a further potential species in the therapy of the recent coronavirus of severe acute respiratory syndrome coronavirus 2 accountable for coronavirus sickness. The physico-chemical qualifications from minimized frame of *apigenine-7-glucoside, catechin, demethoxycurcumine, kaempferol, naringenin, oleuropein* and *quercetin* extracted from *Goji berries, Green tea, Turmeric, Chinese cabbage, Citrus fruit, Olive and Chili pepper*, respectively, revealed to be intensive in depicting antiviral activities by disconnecting the viral habitance. Among applied extracted phytochemicals in this investigation, oleuropein’s has exhibited lowest Gibbs free energy of -1206.893×10^3 kcal/mol with high dipole moment of 6.1962 Debye. Afterwards, these herbal medications might be either a novel and assured cure or even are engaged as antiviral nutraceuticals in raising immunity and tolerance to virus infections. Secondary metabolism is for ecological interactions and a significant source of natural products applied in pharmaceuticals. Through the progress in bioinformatics tools and sequencing technologies, a high number of biosynthetic gene clusters of secondary metabolites have been explored from microbial genomes. But, owing to challenges from the difficulty of genome-scale process rehabilitation on secondary metabolism, the quantitative modeling of secondary metabolism is weakly performed. Modeling approaches will simplify quantitative investigation of secondary metabolism and design of engineering methods for medicinal plant production.

Author contributions: Conceptualization, FM; methodology, FM and MM; software, FM and MM; validation, FM; formal analysis, FM and MM; investigation, FM and MM; resources, MM; data curation, FM and MM; writing—original draft preparation,

FM; writing—review and editing, MM; visualization, FM and MM; supervision, FM; project administration, FM. All authors have read and agreed to the published version of the manuscript.

Acknowledgments: In successfully completing this paper and its research, the authors are grateful to Kastamonu University.

Ethical approval: Not applicable.

Conflict of interest: The authors declare no conflict of interest.

References

1. Zhang J, Zhou L, Yang Y, et al. Therapeutic and triage strategies for 2019 novel coronavirus disease in fever clinics. *Lancet*. 2020; 395: e39. doi: 10.1016/S0140-6736(20)30313-5
2. Salih WA, Al-Taie A. Synthesis and characterization of laser-ablated silver and titanium oxide nanoparticles: Implications for drug delivery. *New Materials, Compounds and Applications*. 2024; 8(2): 199-222. doi:10.62476/nmca82199
3. Yan B, Chu H, Yang D, et al. Characterization of the Lipidomic Profile of Human Coronavirus-Infected Cells: Implications for Lipid Metabolism Remodeling upon Coronavirus Replication. *Viruses*. 2019; 11(1): 73. doi: 10.3390/v11010073
4. Abdullayeva AA, Ahmadova NE, Atakishiyeva GT, et al. Molecular docking of 4-azido-2-(4-substituted-phenyl)-5-(2-nitrophenyl)-2h-1,2,3-triazoles. *New Materials, Compounds and Applications*. 2024; 8(1): 5-12. doi:10.62476/nmca8105
5. Sarasia EM, Afsharnezhad S, Honarparvar B, et al. Theoretical study of solvent effect on NMR shielding tensors of luciferin derivatives. *Physics and Chemistry of Liquids*. 2011; 49(5): 561-571. doi: 10.1080/00319101003698992
6. Mollaamin F. Structural and Functional Characterization of Medicinal Plants as Selective Antibodies towards Therapy of COVID-19 Symptoms. *Antibodies*. 2024; 13(2): 38. doi: 10.3390/antib13020038
7. Mitton B, Rule R, Said M. Laboratory evaluation of the BioFire FilmArray Pneumonia plus panel compared to conventional methods for the identification of bacteria in lower respiratory tract specimens: a prospective cross-sectional study from South Africa. *Diagnostic Microbiology and Infectious Disease*. 2021; 99(2): 115236. doi: 10.1016/j.diagmicrobio.2020.115236
8. Pashayev BG, Aliyev LP, Hajiyeva ShN, Viscous flow and structural properties in water-ethanol-urea systems. *Advanced Physical Research*. 2024; 6(1): 29-35. doi: 10.62476/apr61.35
9. Alzand KI, Younis HR, Salman HD, et al., *New Materials, Compounds and Applications*. 2024; 8(1): 75-86. doi:10.62476/nmca8175
10. Caméléna F, Moy AC, Dudoignon E, et al. Performance of a multiplex polymerase chain reaction panel for identifying bacterial pathogens causing pneumonia in critically ill patients with COVID-19. *Diagnostic Microbiology and Infectious Disease*. 2021; 99(1): 115183. doi: 10.1016/j.diagmicrobio.2020.115183
11. Mollaamin F. Computational Methods in the Drug Delivery of Carbon Nanocarriers onto Several Compounds in Sarraceniaceae Medicinal Plant as Monkeypox Therapy. *Computation*. 2023; 11(4): 84. doi: 10.3390/computation11040084
12. Van TT, Kim TH, Butler-Wu SM. Evaluation of the Biofire FilmArray meningitis/encephalitis assay for the detection of *Cryptococcus neoformans/gattii*. *Clinical Microbiology and Infection*. 2020; 26(10): 1375-1379. doi: 10.1016/j.cmi.2020.01.007
13. Alzand KI, Younis HR, Salman HD, et al. Citrus aurantium L. peels and seeds: Phytochemical screening and antibacterial activity. *New Materials, Compounds and Applications*. 2024; 8(1): 75-86. doi:10.62476/nmca8175
14. Cailleaux M, Pilmis B, Mizrahi A, et al. Impact of a multiplex PCR assay (FilmArray) on the management of patients with suspected central nervous system infections. *European Journal of Clinical Microbiology & Infectious Diseases*. 2019; 39(2): 293-297. doi: 10.1007/s10096-019-03724-7
15. Sheet SHM, Mahmud RB, Saeed NHM, et al. Theoretical study for comparison of pKa of a number of Achiff bases by employing parameters derived from DFT and MP2 method. *New Materials, Compounds and Applications*. 2024; 8(1): 94-108. doi: 10.62476/nmca8194
16. Mollaamin F. Characterizing the structural and physicochemical properties of medicinal plants as a proposal for treating of viral malady. *Trends in Immunotherapy*. 2023; 7(2): 2329. doi: 10.24294/ti.v7.i2.2329
17. Atanasov AG, Zotchev SB, Dirsch VM, et al. Natural products in drug discovery: advances and opportunities. *Nature Reviews Drug Discovery*. 2021; 20(3): 200-216. doi: 10.1038/s41573-020-00114-z

18. Lin LT, Hsu WC, Lin CC. Antiviral Natural Products and Herbal Medicines. *Journal of Traditional and Complementary Medicine*. 2014; 4(1): 24-35. doi: 10.4103/2225-4110.124335
19. Kumar Shakya A, Arvind Kumar Shakya C. Medicinal Plants: Future Source of New Drugs. *International Journal of Herbal Medicine*. 2016.
20. Ibrahim AK, Youssef AI, Arafa AS, et al. Anti-H5N1 virus flavonoids from Capparis sinaica Veill. *Natural Product Research*. 2013; 27(22): 2149-2153. doi: 10.1080/14786419.2013.790027
21. Yarmolinsky L, Huleihel M, Zaccai M, et al. Potent antiviral flavone glycosides from Ficus benjamina leaves. *Fitoterapia*. 2012; 83(2): 362-367. doi: 10.1016/j.fitote.2011.11.014
22. Orhan DD, Özçelik B, Özgen S, et al. Antibacterial, antifungal, and antiviral activities of some flavonoids. *Microbiological Research*. 2010; 165(6): 496-504. doi: 10.1016/j.micres.2009.09.002
23. Riva A, Ronchi M, Petrangolini G, et al. Improved Oral Absorption of Quercetin from Quercetin Phytosome, a New Delivery System Based on Food Grade Lecithin. *European Journal of Drug Metabolism and Pharmacokinetics*. 2018; 44(2): 169-177. doi: 10.1007/s13318-018-0517-3
24. Hakobyan A, Arabyan E, Avetisyan A, et al. Apigenin inhibits African swine fever virus infection in vitro. *Archives of Virology*. 2016; 161(12): 3445-3453. doi: 10.1007/s00705-016-3061-y
25. Huang H, Zhou W, Zhu H, et al. Baicalin benefits the anti-HBV therapy via inhibiting HBV viral RNAs. *Toxicology and Applied Pharmacology*. 2017; 323: 36-43. doi: 10.1016/j.taap.2017.03.016
26. Yanai T, Tew DP, Handy NC. A new hybrid exchange–correlation functional using the Coulomb-attenuating method (CAM-B3LYP). *Chemical Physics Letters*. 2004; 393(1-3): 51-57. doi: 10.1016/j.cplett.2004.06.011
27. Grimme S, Antony J, Ehrlich S, et al. A consistent and accurate ab initio parametrization of density functional dispersion correction (DFT-D) for the 94 elements H-Pu. *The Journal of Chemical Physics*. 2010; 132(15). doi: 10.1063/1.3382344
28. Frisch MJ, Trucks GW, Schlegel HB, et al. Gaussian 16, Revision C.01. Gaussian, Inc., Wallingford CT; 2016.
29. Mirzayeva DM, Aghayeva SA, Kaplina SP, et al. Mechanism of formation water molecules and chemical bonds in Leptothrix materials. *Advanced Physical Research*. 2024; 6(1): 5-14. doi: 10.62476/apr61514
30. Roy TK, Kopysov V, Pereverzev A, et al. Intrinsic structure of pentapeptide Leu-enkephalin: geometry optimization and validation by comparison of VSCF-PT2 calculations with cold ion spectroscopy. *Physical Chemistry Chemical Physics*. 2018; 20(38): 24894-24901. doi: 10.1039/c8cp03989e
31. Monajjemi M, Mollaamin F, Shojaei S. An overview on Coronaviruses family from past to Covid-19: introduce some inhibitors as antiviruses from Gillan's plants. *Biointerface Research in Applied Chemistry*. 2020; 10(3): 5575-5585. doi: 10.33263/briac103.575585
32. Zadeh MAA, Lari H, Kharghanian L, et al. Density Functional Theory Study and Anti-Cancer Properties of Shyshaq Plant: In View Point of Nano Biotechnology. *Journal of Computational and Theoretical Nanoscience*. 2015; 12(11): 4358-4367. doi: 10.1166/jctn.2015.4366
33. Dawoud RA, Shehata RS, Moawod H, et al. Impact of bio-organic fertilization and nitrogen levels on maize (*Zea mays* L.) resilience. *New Materials, Compounds and Applications*. 2024; 8(1): 43-61. doi:10.62476/nmca8143
34. Demukhamedova SD, Aliyeva IN. Computer simulation of the structure of some azo-derivatives of β -diketones by the methods of quantum chemistry. *New Materials, Compounds and Applications*. 2024; 8(1): 24-42. doi: 10.62476/nmca8124
35. Ni W, Li G, Zhao J, et al. Use of Monte Carlo simulation to evaluate the efficacy of tigecycline and minocycline for the treatment of pneumonia due to carbapenemase-producing *Klebsiella pneumoniae*. *Infectious Diseases*. 2018; 50(7): 507-513. doi: 10.1080/23744235.2018.1423703
36. Mollaamin F. Physicochemical investigation of anti-covid19 drugs using several medicinal plants. *Journal of the Chilean Chemical Society*. 2022; 67(2): 5537-5546. doi: 10.4067/s0717-97072022000205537
37. McArdle S, Mayorov A, Shan X, et al. Digital quantum simulation of molecular vibrations. *Chemical Science*. 2019; 10(22): 5725-5735. doi: 10.1039/c9sc01313j
38. Eberhardt J, Santos-Martins D, Tillack A, et al. AutoDock Vina 1.2.0: New Docking Methods, Expanded Force Field, and Python Bindings. *Journal of Chemical Information and Modeling*. 2021.
39. Ezzat MO, Razik BMA, Shihab WA. Molecular modelling and theoretical design of novel nirmatrelvir derivatives as SARS-CoV-2 entry inhibitors. *New Materials, Compounds and Applications*. 2024; 8(2): 178-189. doi:10.62476/nmca82178.

40. Kawczak P, Bober L, Bączek T. QSAR Analysis of Selected Antimicrobial Structures Belonging to Nitro-derivatives of Heterocyclic Compounds. *Letters in Drug Design & Discovery*. 2020; 17(2): 214-225. doi: 10.2174/1570180815666181004112947
41. Ibrahimova SA, Mukhtarova SH, Eyvazova SM, et al. Prediction of biological activity by means of synthesis and QSAR model of phenylhydrazone based on methyl 4-formylbenzoate. *New Materials, Compounds and Applications*. 2024; 8 (3): 373-389. doi:10.62476/nmca83373
42. Eisenreich W, Leberfing J, Rudel T, et al. Interactions of SARS-CoV-2 with Human Target Cells—A Metabolic View. *International Journal of Molecular Sciences*. 2024; 25(18): 9977. doi: 10.3390/ijms25189977
43. Yadav R, Chaudhary JK, Jain N, et al. Role of Structural and Non-Structural Proteins and Therapeutic Targets of SARS-CoV-2 for COVID-19. *Cells*. 2021; 10(4): 821. doi: 10.3390/cells10040821
44. Justo Arevalo S, Castillo-Chávez A, Uribe Calampa CS, et al. What do we know about the function of SARS-CoV-2 proteins?. *Frontiers in Immunology*. 2023; 14. doi: 10.3389/fimmu.2023.1249607
45. Srinivasan V, Brognaro H, Prabhu PR, et al. Antiviral activity of natural phenolic compounds in complex at an allosteric site of SARS-CoV-2 papain-like protease. *Communications Biology*. 2022; 5(1). doi: 10.1038/s42003-022-03737-7
46. Kumar K, Debnath P, Singh S, et al. An Overview of Plant Phenolics and Their Involvement in Abiotic Stress Tolerance. *Stresses*. 2023; 3(3): 570-585. doi: 10.3390/stresses3030040
47. Orfali R, Rateb ME, Hassan HM, et al. Sinapic Acid Suppresses SARS CoV-2 Replication by Targeting Its Envelope Protein. *Antibiotics*. 2021; 10(4): 420. doi: 10.3390/antibiotics10040420
48. Goc A, Sumera W, Rath M, et al. Phenolic compounds disrupt spike-mediated receptor-binding and entry of SARS-CoV-2 pseudo-virions. *PLOS ONE*. 2021; 16(6): e0253489. doi: 10.1371/journal.pone.0253489
49. Tirado-Kulieva VA, Hernández-Martínez E, Choque-Rivera TJ. Phenolic compounds versus SARS-CoV-2: An update on the main findings against COVID-19. *Heliyon*. 2022; 8(9): e10702. doi: 10.1016/j.heliyon.2022.e10702
50. Montenegro-Landívar MF, Tapia-Quirós P, Vecino X, et al. Polyphenols and their potential role to fight viral diseases: An overview. *Science of The Total Environment*. 2021; 801: 149719. doi: 10.1016/j.scitotenv.2021.149719
51. Kim HK, Choi YH, Verpoorte R. NMR-based metabolomic analysis of plants. *Nature Protocols*. 2010; 5(3): 536-549. doi: 10.1038/nprot.2009.237
52. Safarov JE, Sultanova ShA, Mambetsheripova AA, et al. Mathematical modelling of drying process. *Advanced Physical Research*. 2024; 6(3): 255-262. doi: 10.62476/apr63255
53. Nur Siti Fatimah WO, Deden Saprudin D, Hamim Hamim H. Profile of Secondary Metabolites and Metal in *Jatropha curcas* L. and *Reutealis trisperma* Plants Grown in the Media Contaminated by Gold Mining Tailings using LC-MS/MS. *Materials International*. 2024; 6(1): 6. doi:10.33263/Materials61.006
54. Trontelj Z, Pirnat J, Jazbinšek V, et al. Nuclear Quadrupole Resonance (NQR)—A Useful Spectroscopic Tool in Pharmacy for the Study of Polymorphism. *Crystals*. 2020; 10(6): 450. doi: 10.3390/cryst10060450
55. Sciotto R, Ruiz Alvarado IA, Schmidt WG. Substrate Doping and Defect Influence on P-Rich InP(001): H Surface Properties. *Surfaces*. 2024; 7(1): 79-87. doi: 10.3390/surfaces7010006
56. Luo J, Wang C, Wang Z, et al. NMR and NQR studies on transition-metal arsenide superconductors LaRu₂As₂, KCa₂Fe₄As₄F₂, and A₂Cr₃As₃*. *Chinese Physics B*. 2020; 29(6): 067402. doi: 10.1088/1674-1056/ab892d
57. Smith JAS. Nuclear quadrupole resonance spectroscopy. General principles. *Journal of Chemical Education*. 1971; 48(1): 39. doi: 10.1021/ed048p39
58. Garroway AN. Appendix K: Nuclear quadrupole resonance. In: Jacqueline MacDonald, J. R. Lockwood: *Alternatives for Landmine Detection*. Report MR-1608, Rand Corporation; 2003.
59. Poleshchuck OK, Kalinna EL, Latosinska JN, Koput J. Application of density functional theory to the analysis of electronic structure and quadrupole interaction in dimers of transition and non-transition elements. *Journal of Molecular Structure: Theochem*. 2001; 547 (1-3): 233-243. doi: 10.1016/S0166-1280(01)00636-4
60. Young HA, Freedman RD. *Sears and Zemansky's University Physics with Modern Physics*, 13th ed. Boston: Addison-Wesley; 2012.
61. Abbasi M, Mansourian M, Oskouie AA, et al. In-silico study MM/GBSA binding free energy and molecular dynamics simulation of some designed remdesivir derivatives as the inhibitory potential of SARS-CoV-2 main protease. *Research in Pharmaceutical Sciences*. 2024; 19(1): 29-41. doi: 10.4103/1735-5362.394818